NACA

RESEARCH MEMORANDUM

AERODYNAMIC CHARACTERISTICS AT SUBSONIC AND TRANSONIC SPEEDS OF A 42.7° SWEPTBACK WING MODEL HAVING AN AILERON WITH FINITE TRAILING-EDGE THICKNESS

By

Thomas R. Turner, Vernard E. Lockwood,
and Raymond D. Vogler

Langley Aeronautical Laboratory
Langley Field, Va.

NATIONAL ADVISORY COMMITTEE
FOR AERONAUTICS

WASHINGTON

January 12, 1949

NACA RM No. L8K02

NATIONAL ADVISORY COMMITTEE FOR AERONAUTICS

RESEARCH MEMORANDUM

AERODYNAMIC CHARACTERISTICS AT SUBSONIC AND TRANSONIC SPEEDS OF A 42.7° SWEPTBACK WING MODEL HAVING AN AILERON WITH FINITE TRAILING-EDGE THICKNESS

By Thomas R. Turner, Vernard E. Lockwood, and Raymond D. Vogler

SUMMARY

An investigation at subsonic and transonic speeds has been performed in the Langley high-speed 7- by 10-foot tunnel to determine the aerodynamic characteristics of a 42.7° sweptback wing with a 20-percent-chord and 50-percent-span outboard aileron. The model had a circular-arc airfoil section and the aileron trailing-edge thickness was modified for the different tests. The investigation was performed in transonic flow over a bump on the tunnel floor and in subsonic flow on one of the tunnel side walls. The Mach number for this investigation varied from about 0.42 to 1.17 and the Reynolds number varied from 800,000 to 1,220,000.

The data presented indicate that changing the circular-arc aileron contour to a flat-sided aileron contour with finite trailing-edge thickness eliminated reversal of control in most cases and generally improved the aileron control characteristics. The drag coefficient was increased and the aerodynamic center shifted rearward in the subsonic Mach number range.

INTRODUCTION

One of the many problems arising from the use of high-speed aircraft has been that of securing adequate lateral control, particularly in the transonic speed range. An investigation has been made (reference 1) to determine the aileron control characteristics of a 42.7° sweptback circular-arc wing with various ailerons through a Mach number range from 0.5 to 1.2 by using the transonic bump. The original circular-arc contour aileron gave very low effectiveness in the transonic speed range and the effectiveness reversed for some conditions. An aileron having flat sides and a trailing edge the same thickness as the aileron thickness at the hinge line gave reasonable effectiveness and showed no reversal of effectiveness up to a Mach number of 1.2 (reference 1).

The purpose of this investigation was to determine the rolling-moment characteristics of the model of reference 1 with an aileron having flat sides and a trailing-edge thickness less than the thickness at the hinge line, up to a Mach number of 1.17. Lift and drag characteristics were obtained up to a Mach number of 1.15 and the pitching-moment characteristics, up to a Mach number of 0.95.

SYMBOLS AND CORRECTIONS

C_L	lift coefficient $\left(\frac{L}{\frac{1}{2}qS}\right)$
C_D	drag coefficient $\left(\frac{D}{\frac{1}{2}qS}\right)$
C_m	pitching-moment coefficient $\left(\frac{M'}{\frac{1}{2}qS\bar{c}}\right)$
C_{l_a}	rolling-moment coefficient produced by aileron $\left(\frac{L'}{qSb}\right)$
L	lift, pounds
D	drag, pounds
M'	pitching moment about 0.183 mean geometric chord, foot-pounds
L'	rolling-moment produced by aileron about plane of symmetry, foot-pounds
S	twice area of semispan model (0.25 sq ft)
b	twice span of semispan model (1 ft)
$\bar{c}$	wing mean geometric chord (0.259 ft)
t	ratio of aileron thickness at trailing edge to thickness at hinge line
α	angle of attack, degrees
δ_a	aileron deflection, positive when trailing edge is down, degrees
q	average dynamic pressure over span of model, pounds per square foot $\left(\frac{1}{2}\rho V^2\right)$

[redacted]

ρ	mass density of air, slugs per cubic foot
V	air velocity, feet per second
M	average Mach number over span of model
M_T	tunnel reference Mach number
M_l	local Mach number
R	Reynolds number

The rolling-moment data have been corrected in accordance with the method of reference 2 for reflection-plane models. This correction is for extremely low Mach numbers. No correction has been made for Mach number effect. The correction applied was as follows:

$$c_{l_a} = 0.897 c_{l_{measured}}$$

All data are presented about the wind axes.

MODEL

The semispan wing model for these tests had a leading-edge sweepback of 42.7°, a taper ratio of 0.50, and an aspect ratio of 4.0; other geometric characteristics are shown in figure 1. The wing, made of steel with a polished surface, had a 10-percent-thick circular-arc section normal to the 50-percent-chord line, had no dihedral, and was mounted as a midwing (fig. 1). The polished-brass fuselage was semicircular in cross section and was bent to the contour of the bump. The fuselage for the tests on the side wall of the tunnel was made of hardwood.

The 50-percent-span outboard aileron was attached to the wing with a $\frac{1}{32}$-inch-thick copper insert (fig. 1). This insert was bent to obtain the required aileron deflection. The deflection was checked before and after each test. The various aileron profiles investigated are shown in figure 2. The aileron chord was 20 percent of the wing chord.

TEST TECHNIQUE

The tests were performed in the Langley high-speed 7- by 10-foot tunnel which is capable of reaching the choking Mach number. In order to obtain transonic speeds in the tunnel, an application of the NACA wing-flow method of testing was made (reference 3). This method of testing at transonic speeds involves placing the model in the high-velocity

[redacted]

flow field generated over the curved surface of a bump on the tunnel floor (fig. 3). A sketch showing the location of the model on the bump is given in figure 4. An electrical strain-gage balance was mounted in a chamber in the bump to measure the aerodynamic forces and moments of the model. The chamber is sealed except for a hole through which the butt of the wing passes. The fuselage which was approximately $\frac{1}{32}$ inch above the bump surface covered this hole.

The chordwise variation of Mach number along the surface of the bump is shown in figure 5. This figure also presents the vertical variation of Mach number at a chordwise station 12 inches from the leading edge of the bump. It should be noted that at a given tunnel Mach number the local Mach number obtained from surface static pressure measurements at station 12 is somewhat higher than the maximum value indicated from the vertical survey (fig. 5). This difference in Mach number is brought about by not taking into account the total pressure loss in the boundary layer for the surface survey. Extrapolation of the vertical survey to the surface of the bump gives nearly the same Mach number as is obtained from the surface survey. The test Mach number was the average Mach number over the span of the model. The average Mach number over the span of the model is higher than the average Mach number over the span of the aileron by approximately 0.01 at the lowest Mach number and 0.03 at the highest Mach number tested (fig. 5). No attempt has been made to evaluate the effect of the variation in Mach number along the chord and span of the model.

Mechanical difficulty with the balance used in the bump made it necessary to conduct part of the investigation at subsonic speeds on the wall of the Langley high-speed 7- by 10-foot tunnel by means of the setup shown in figure 6. The reflection plane was spaced out from the tunnel wall to situate the model out of the tunnel boundary layer. The Mach number did not vary over 1 percent over the chord and span of the model for these tests.

The variation of Reynolds number of the model with Mach number for average conditions is presented in figure 7.

RESULTS AND DISCUSSIONS

Wing-Fuselage Aerodynamic Characteristics

The lift and drag characteristics of the model obtained from the transonic bump are presented in figures 8 and 9, respectively. The subsonic lift, drag, and pitching-moment characteristics for the model obtained from the wall mount are presented in figures 10 to 14. In general, the results from the two methods are in good agreement.

The variation of lift coefficient with Mach number at several angles of attack for the aileron with $t = 0$ (circular arc), $t = 0.50$ (flat sides), and $t = 1.00$ (flat sides) is presented in figure 8. From these data it appears that the variation of lift coefficient with Mach number is practically unaffected by the various aileron profiles tested. The variation of lift coefficient with angle of attack for several subsonic Mach numbers is presented in figures 10 to 12. At a Mach number of 0.607 the lift-curve slope near an angle of attack of 0° is less than the slope at larger angles of attack; however, at higher Mach numbers the slope becomes more nearly linear through the test angle-of-attack range. The low Reynolds number at which this investigation was made is probably responsible for part of the nonlinearity of the lift curves near zero lift.

The drag characteristics for the model with circular-arc aileron ($t = 0$) are shown in figures 10 and 13. At subcritical speeds the drag coefficient at an angle of attack of 0° is nearly constant at a value of about 0.011. The drag rise for this model configuration comes at a Mach number of approximately 0.90. Increments of drag coefficients ΔC_D resulting from changes in aileron contour are presented in figure 9, for Mach numbers between 0.50 and 1.15. The flat-sided aileron, ($t = 0.50$) shows a small increase in drag coefficient (0.002) over the circular-arc contour aileron below a Mach number of 1.05. Above a Mach number of 1.05 the values of ΔC_D become negative. As might be expected, the flat-sided aileron ($t = 1.00$) gave greater drag coefficients, approximately 0.006 at subsonic Mach numbers, than the circular-arc aileron ($t = 0$) through the Mach number range tested.

The pitching-moment characteristics for the various aileron modifications investigated are presented in figures 10 to 14. These results are summarized in the following table:

Aileron contour	M	Aerodynamic-center location (percent $\bar{c}$)		
		$C_L = -0.2$	$C_L = 0$	$C_L = 0.2$
Circular-arc	0.607	18	-7	18
Circular-arc	.941	--	41	25
Flat-sided, $t = 0.50$	.607	24	9	20
Flat-sided, $t = 0.50$	.934	--	30	30
Flat-sided, $t = 1.00$	.597	29	21	24
Flat-sided, $t = 1.00$	.965	--	38	38

[redacted]

It can be seen from the preceding table that aileron contour had a considerable effect on the aerodynamic-center location of the model at subsonic Mach numbers. Thickening the aileron trailing edge shifted the aerodynamic center rearward by approximately 2 to 10 percent at a subcritical Mach number of approximately 0.60 at lift coefficients of 0.20 and -0.2. The jog in the pitching-moment-coefficient curve near zero lift for the circular-arc contour aileron (fig. 10) is equivalent to about a 25-percent forward shift in the aerodynamic-center location. This forward shift of the aerodynamic-center location for the flat-sided aileron (fig. 11) near zero lift is approximately 11 percent. These jogs may have been accentuated by the relatively low test Reynolds numbers. However, inasmuch as this forward shift in aerodynamic center occurs within a very small lift range (about $0.05C_L$), it is thought that it will result in no serious stability or control problems.

Above the critical Mach number for this model there is a considerable rearward shift of the aerodynamic-center position. However, the limited amount of data obtained does not justify any conclusions concerning the effect of aileron contour.

Aileron Control Characteristics

The results of the investigation of the aileron control characteristics for the various aileron contours are shown in figures 15 to 19. The rolling-moment coefficients of the aileron with circular-arc ($t = 0$) and flat-sided ($t = 1.00$) contour presented in reference 1 are reproduced in figures 15 and 16 for comparison with additional data on the aileron with other trailing-edge thicknesses ($t = 0.37$ and 0.50) in figures 17 and 18.

From the rolling-moment-coefficient data presented in figure 17 it appears that the aileron with a value of $t = 0.50$ will give control throughout the Mach number range tested. However, at an angle of attack of 3.4° (fig. 17(b)) the aileron effectiveness is very low. The rolling-moment characteristics of the aileron with a value of $t = 0.37$ (fig. 18) appear to be less satisfactory than either of the other ailerons with thickened trailing edges because of very low effectiveness and reversal for $\delta_a = -5^\circ$ and $\alpha = 3.5^\circ$ at a Mach number of 1.15 (fig. 18(b)).

A summary of the effects of aileron profile on the rolling-moment coefficients is presented in figure 19. The aileron with thick trailing edges gave greater values of $\partial C_{l_a}/\partial \delta_a$ than the circular-arc aileron. The aileron with a ratio of trailing-edge thickness to hinge-line thickness of 0.50 shows the most linear variation of C_{l_a} with δ_a of the four aileron-contour configurations investigated and, in addition, the effectiveness $\left(\partial C_{l_a}/\partial \delta_a\right)$ is very near the maximum value obtained for any of the aileron contours investigated.

[redacted]

CONCLUSIONS

Comparative tests of aileron-contour modifications at subsonic and transonic speeds on a 42.7° sweptback circular-arc wing indicated the following conclusions:

1. The aileron showed greater effectiveness with flat sides and thickened trailing edge than it did with circular-arc contour throughout the Mach number range tested. At an angle of attack of 0° there was no indication of reversal of control of the aileron with the trailing edge one-half as thick or as thick as the aileron at the hinge line throughout the Mach number range tested. The aileron with flat sides and trailing edge one-half as thick as the aileron at the hinge line gave the most linear variation of rolling-moment coefficient with aileron deflection at any Mach number and generally gave the highest effectiveness of any configuration investigated.

2. The drag coefficient was increased by thickening the aileron trailing edge at subsonic Mach numbers, but a decrease was indicated in some cases in the transonic range.

3. Thickening the aileron trailing edge shifted the aerodynamic center rearward by approximately 2 to 10 percent at subcritical Mach numbers.

Langley Aeronautical Laboratory
National Advisory Committee for Aeronautics
Langley Field, Va.

[redacted]

REFERENCES

1. Turner, Thomas R., Lockwood, Vernard E., and Vogler, Raymond D.: Preliminary Investigation of Various Ailerons on a 42° Sweptback Wing for Lateral Control at Transonic Speeds. NACA RM No. L8D21, 1948.

2. Swanson, Robert S., and Toll, Thomas H.: Jet-Boundary Corrections for Reflection-Plane Models in Rectangular Wind Tunnels. NACA Rep. No. 770, 1943.

3. Gilruth, R. R., and Wetmore, J. W.: Preliminary Tests of Several Airfoil Models in the Transonic Speed Range. NACA ACR No. L5E08, 1945.

[redacted]

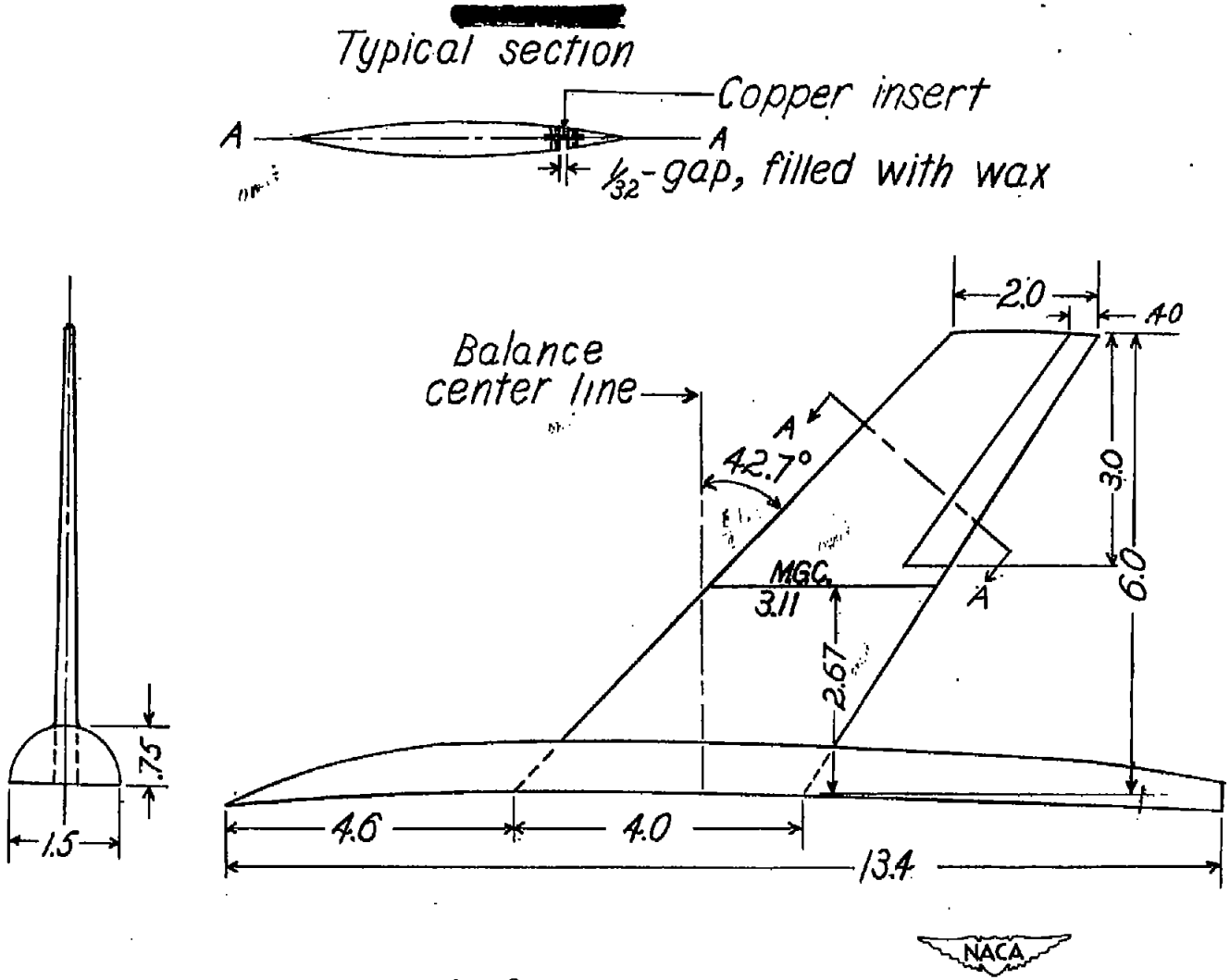

Figure 1.- Drawing of the 42.7° sweptback wing and fuselage combination.
All dimensions in inches.

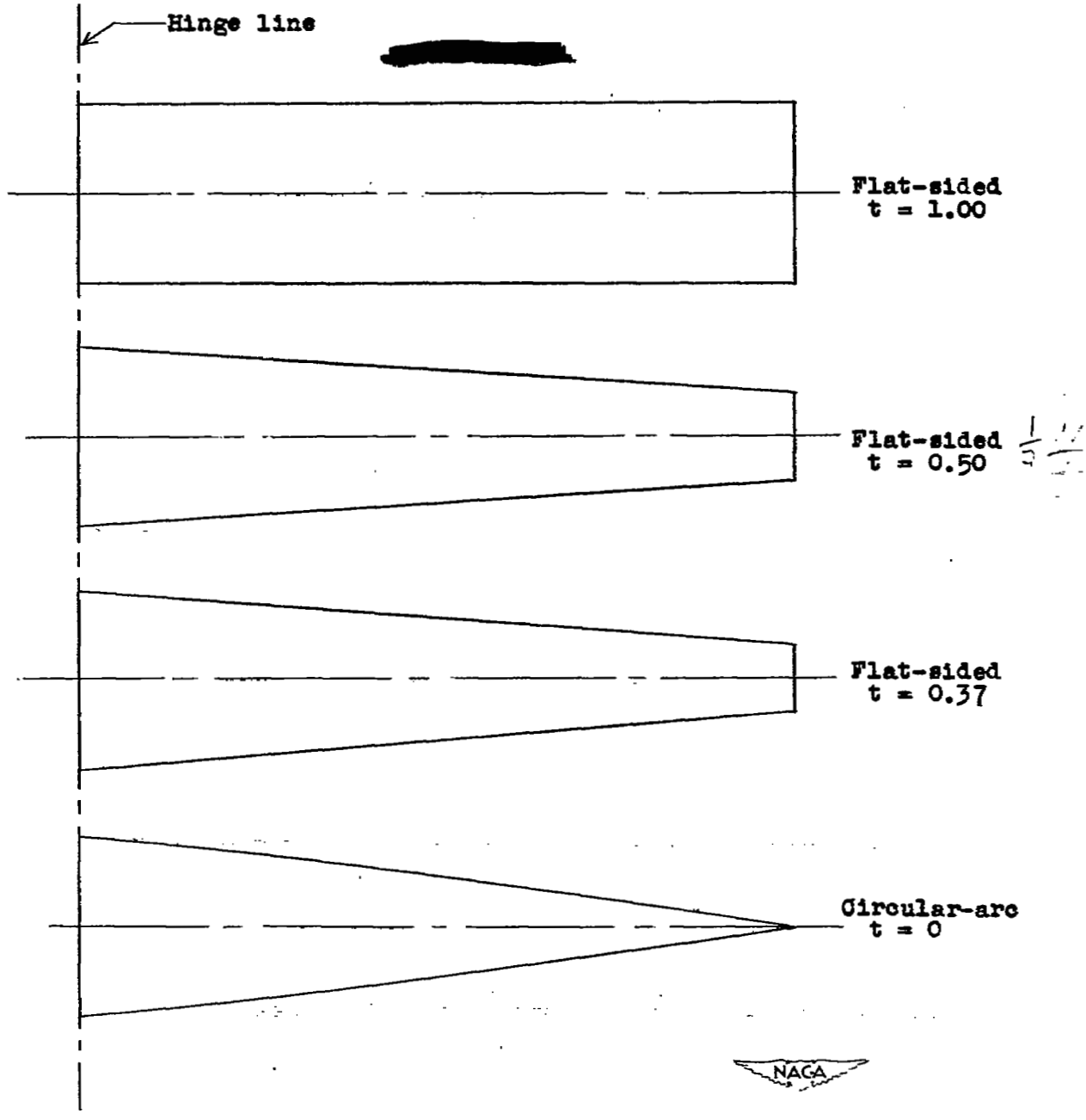

Figure 2.- Section profiles of the 0.20c aileron tested.

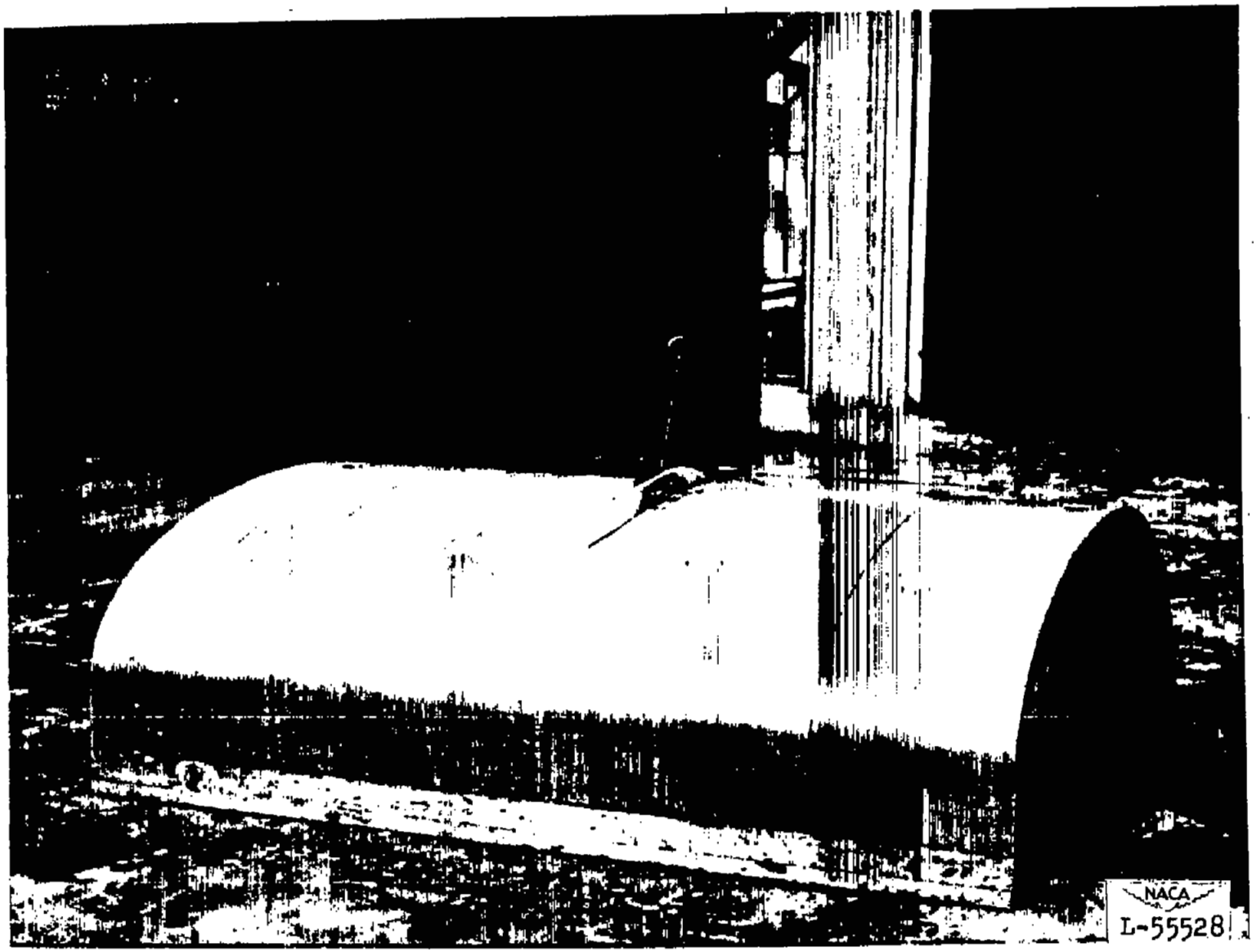

Figure 3.- Three-quarter front view of the model as mounted on the bump in the Langley high-speed 7- by 10-foot tunnel.

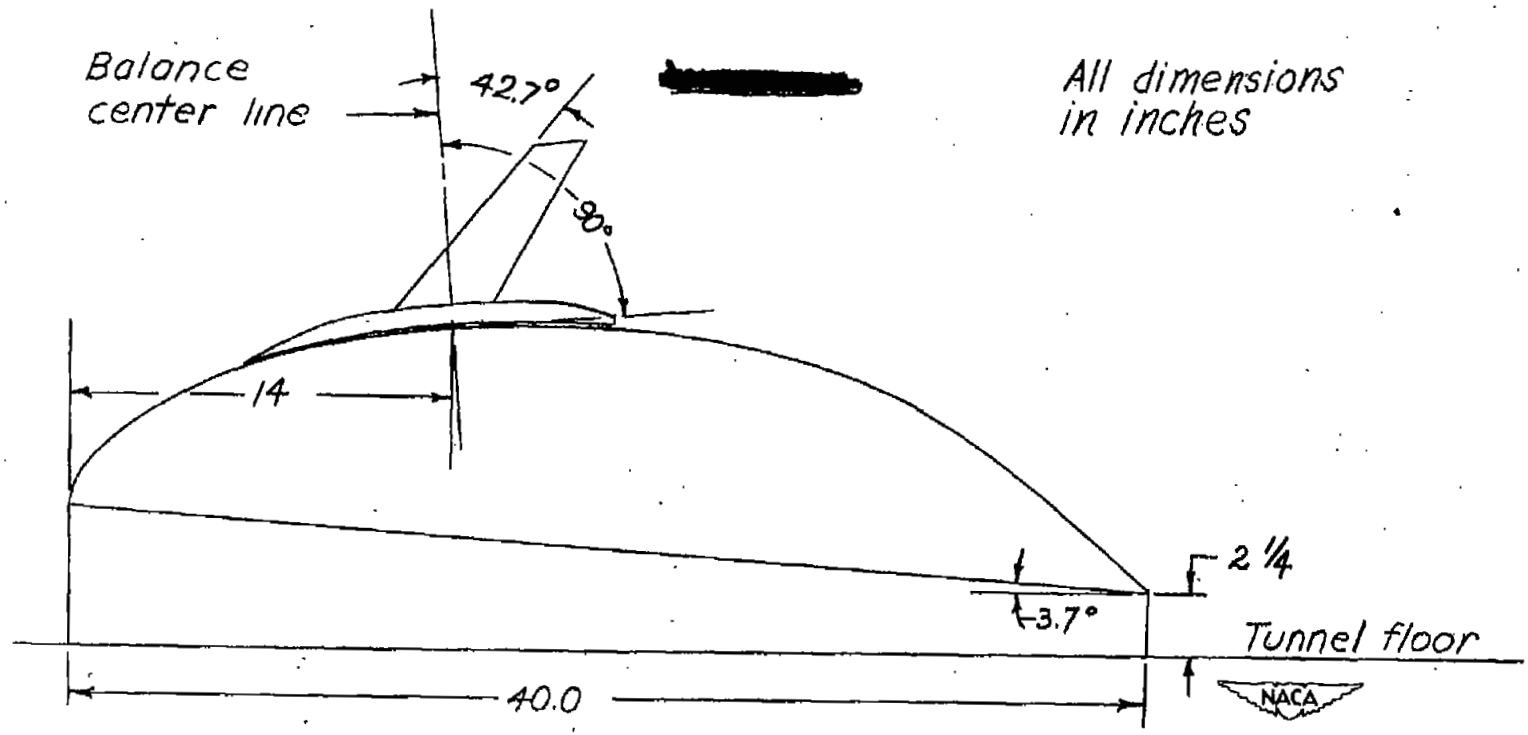

Figure 4.- Schematic sketch of relative position of model, balance, and transonic bump as mounted in the Langley high-speed 7- by 10-foot tunnel.

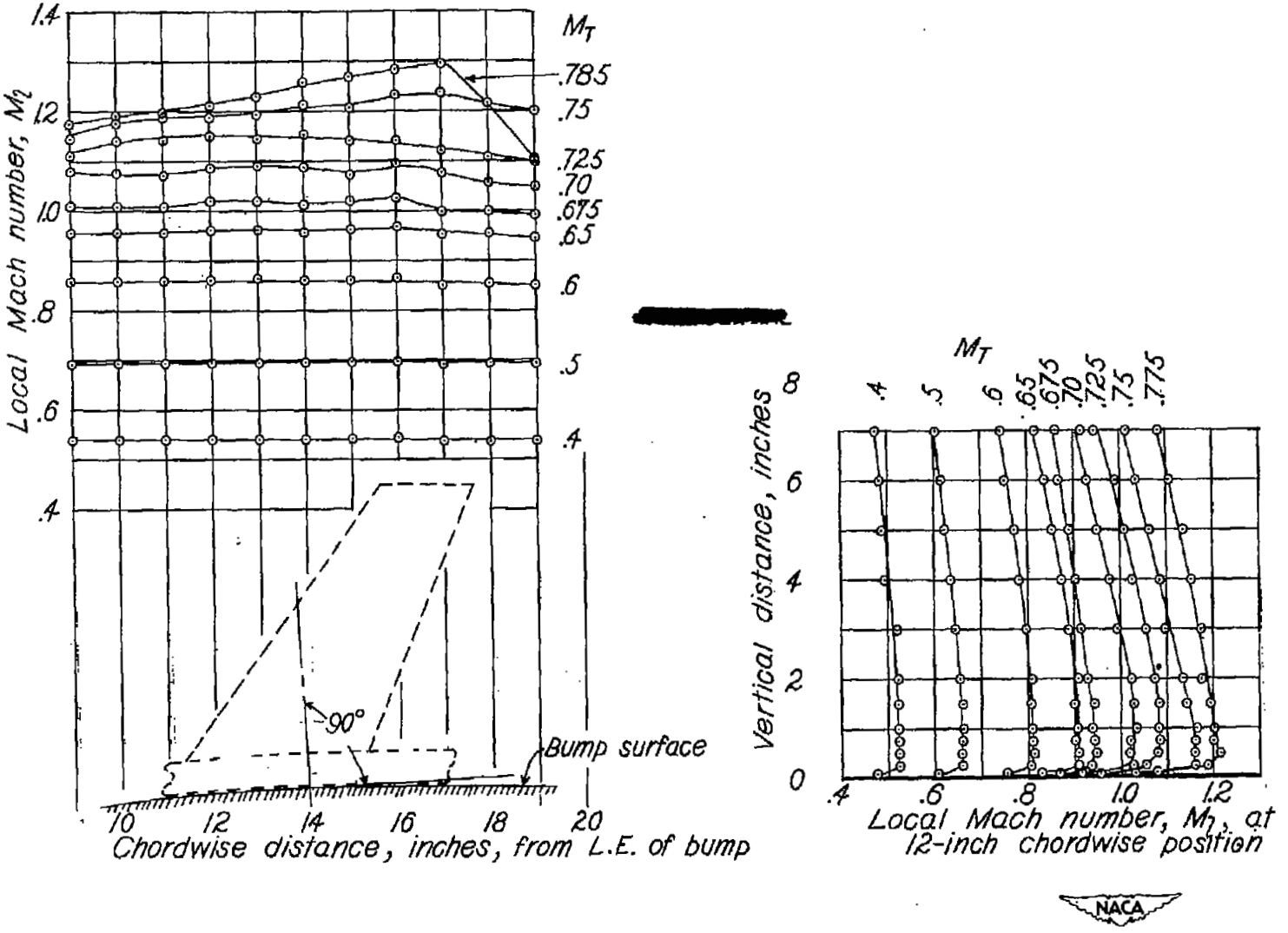

Figure 5.- Spanwise and chordwise distribution of Mach number over transonic bump. Model off.

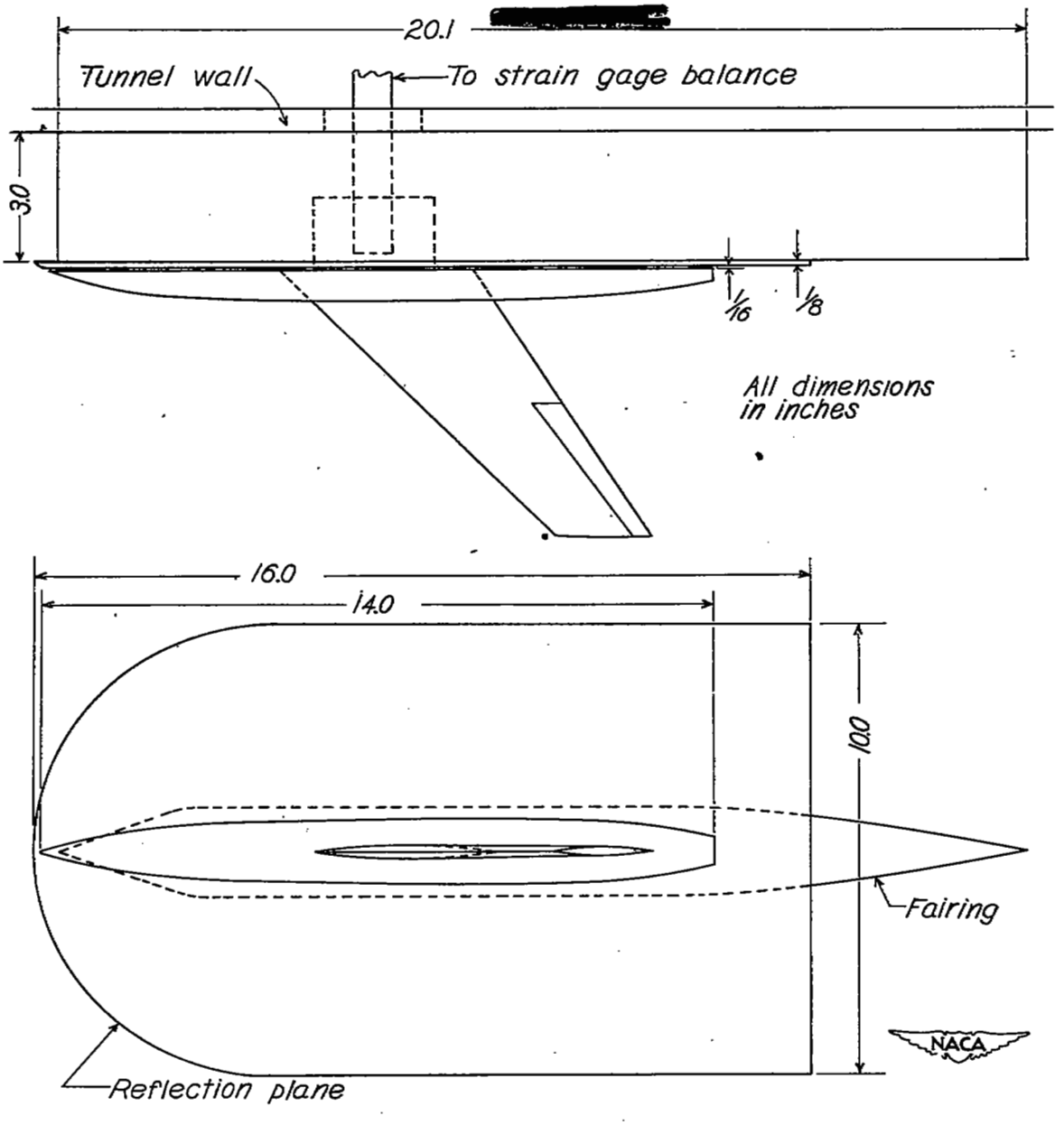

Figure 6.- Drawing of reflection-plane mounting of model on vertical wall of the Langley high-speed 7- by 10-foot tunnel.

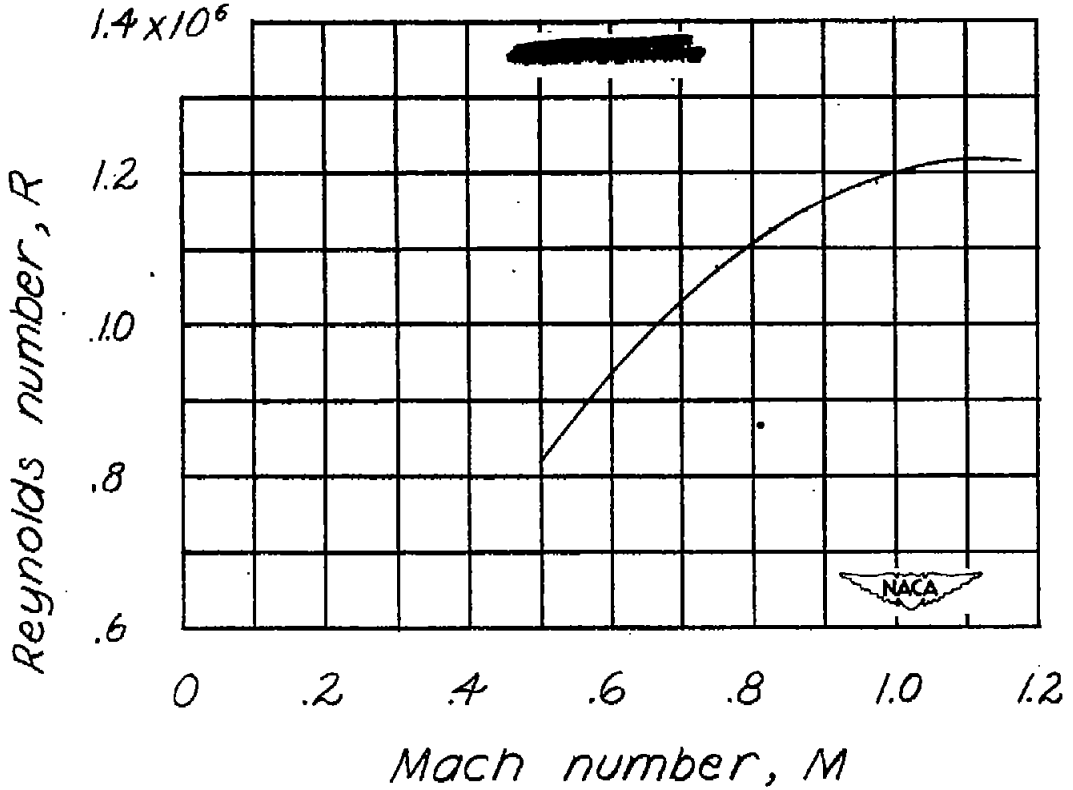

Figure 7.- Variation of Reynolds number with test Mach number. Reynolds number based on model mean geometric chord of 0.25 foot.

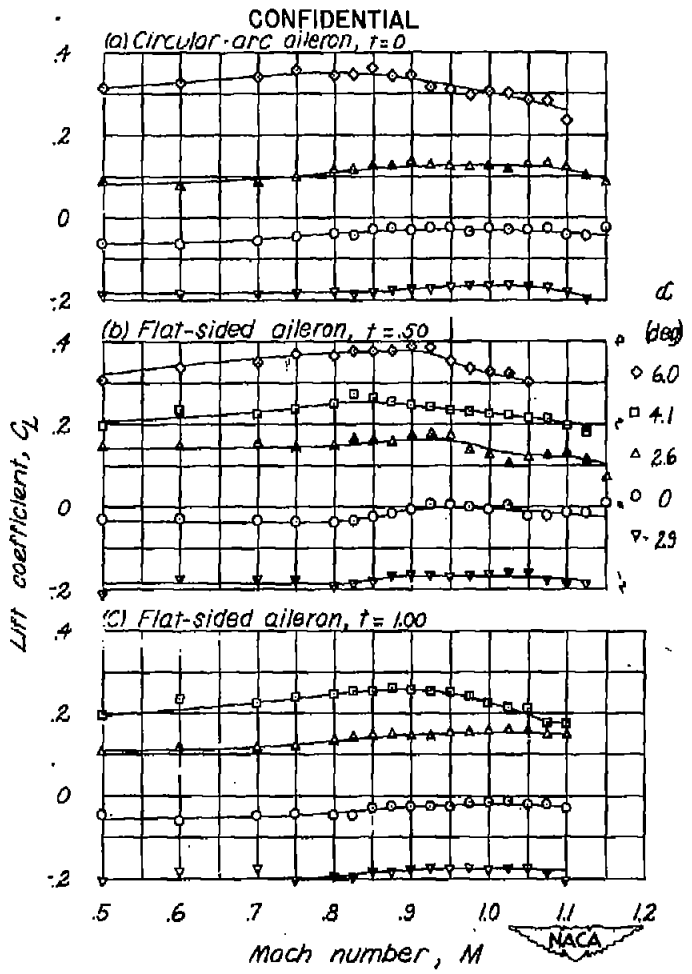

Figure 8.- Variation of lift coefficient with Mach number for the model with several aileron profiles. Data from transonic bump.

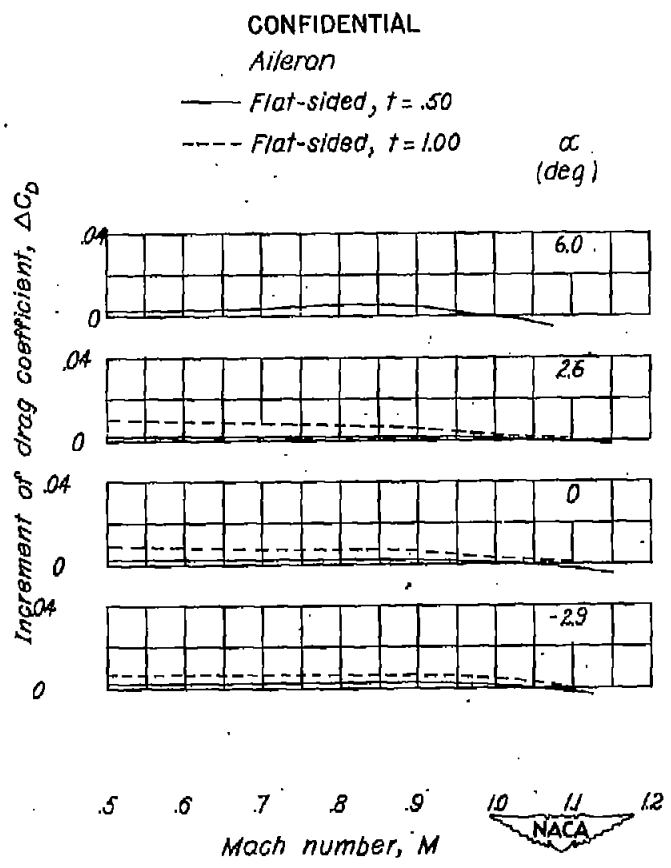

Figure 9.- Variation with Mach number of increment of drag coefficient caused by changing aileron contour from circular arc. Data from transonic bump.

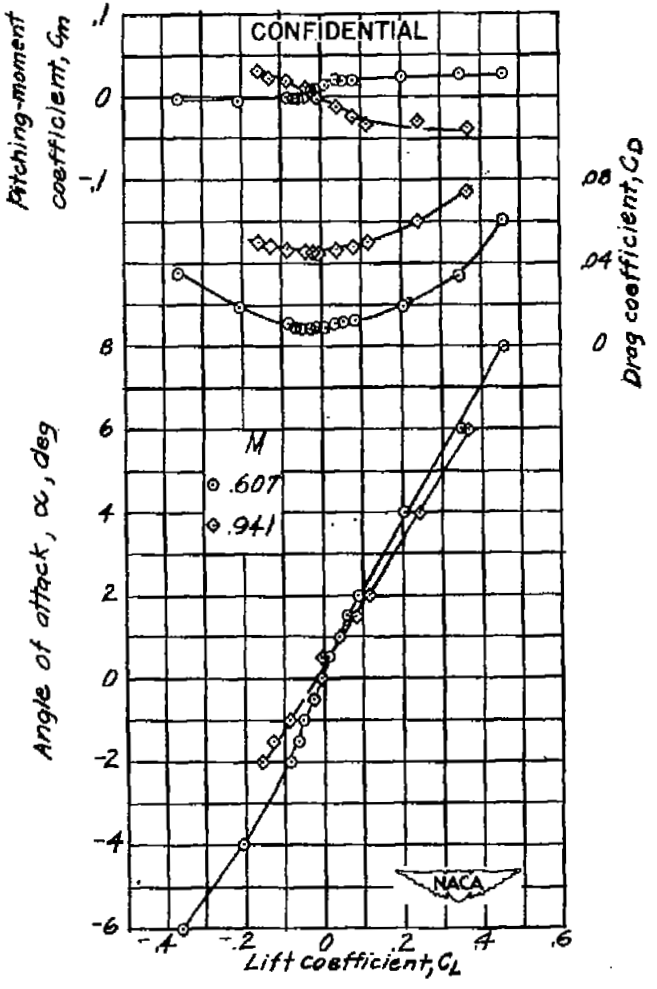

Figure 10.- Aerodynamic characteristics of the model with circular-arc contour aileron. $\delta_a = 0^\circ$.

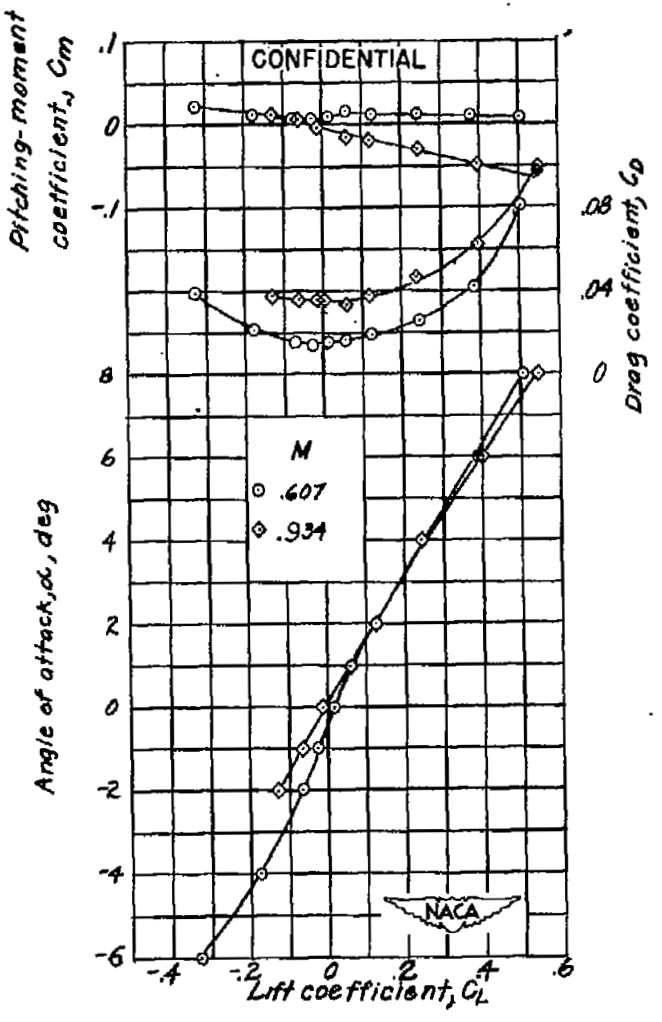

Figure 11.- Aerodynamic characteristics of the model with flat-sided aileron. $t = 0.50$; $\delta_a = 0^\circ$.

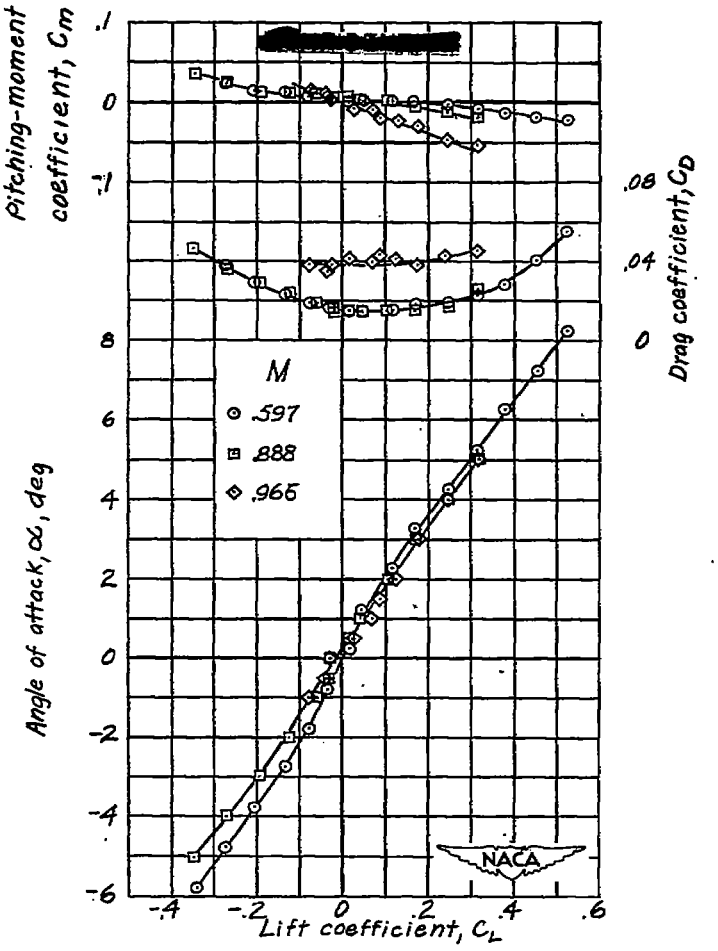

Figure 12.- Aerodynamic characteristics of the model with flat-sided aileron. t = 1.00; $\delta_a = 0^\circ$.

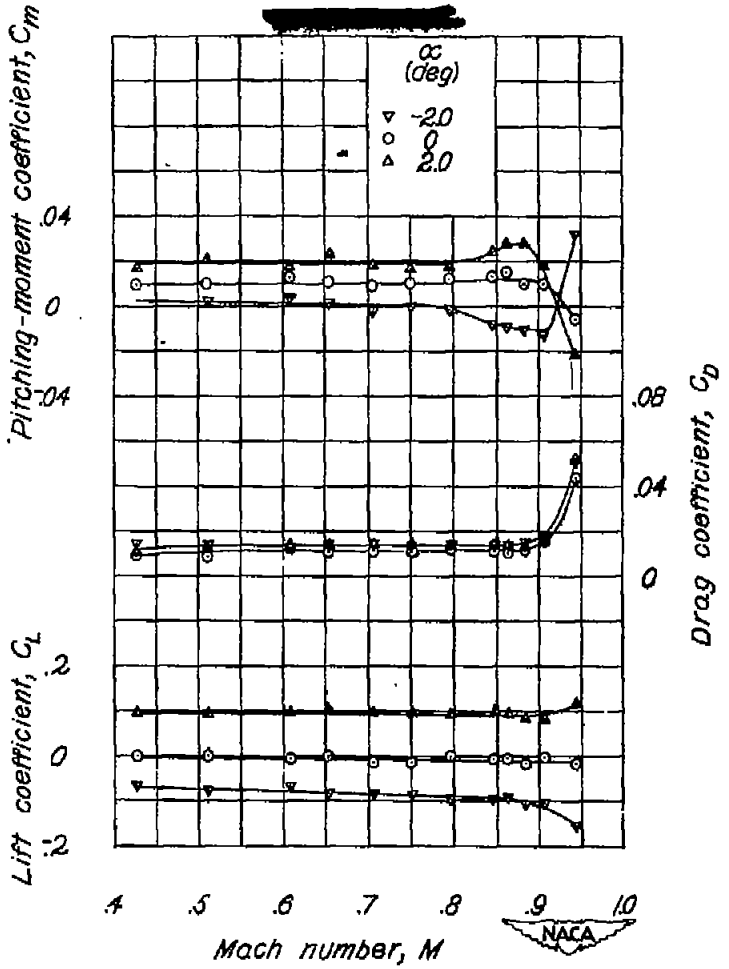

Figure 13.- Variation of the aerodynamic characteristics of the model with Mach number. Circular-arc aileron; $\delta_a = 0^\circ$.

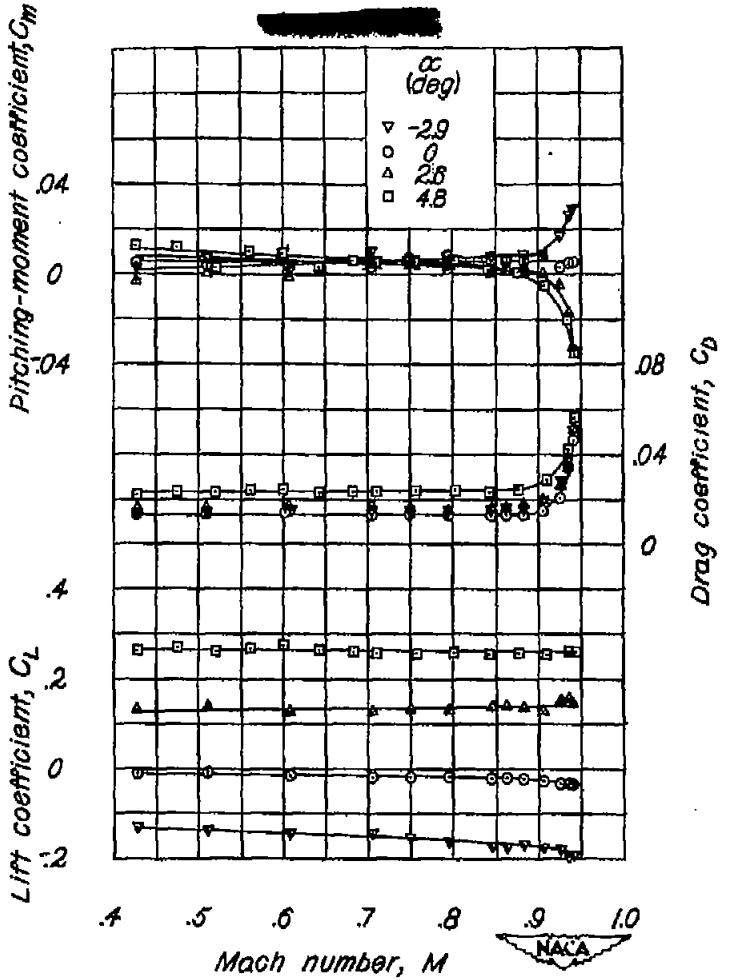

Figure 14.- Variation of the aerodynamic characteristics of the model with Mach number. Flat-sided aileron; $t = 0.50$; $\delta_a = 0^\circ$.

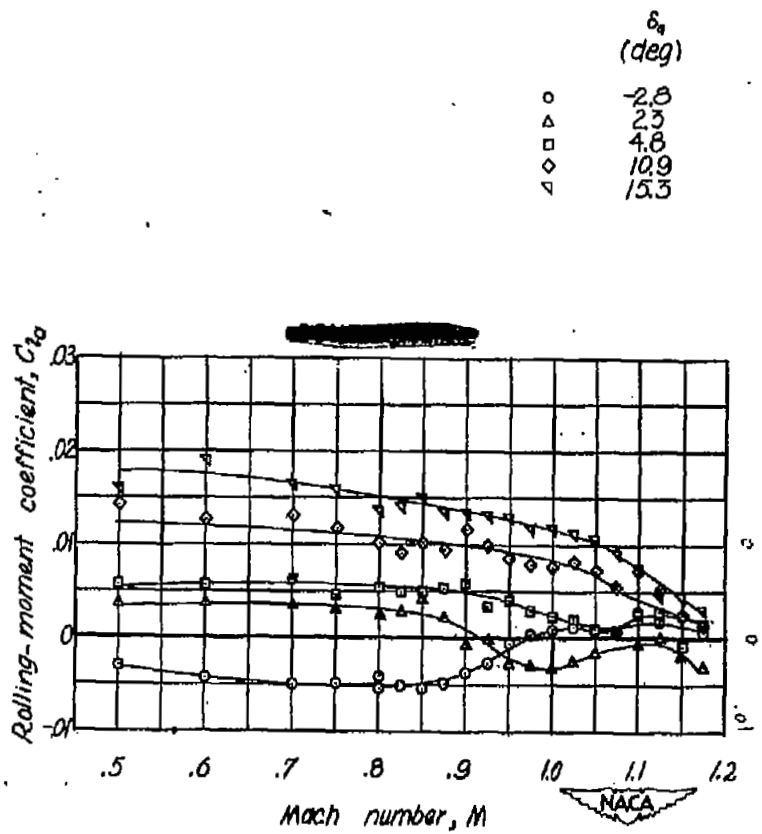

Figure 15.- Variation of rolling-moment coefficient with Mach number for a 0.20-chord circular-arc aileron. $t = 0$; $\alpha = 0^\circ$; data from transonic bump.

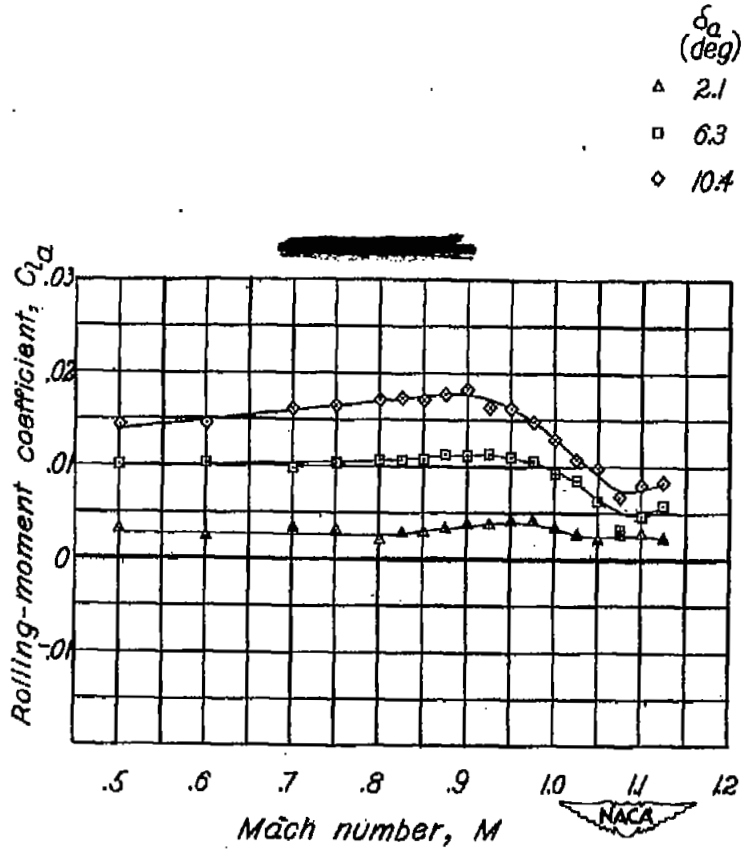

Figure 16.- Variation of rolling-moment coefficient with Mach number for a 0.20-chord flat-sided aileron. $t = 1.00$; $\alpha = 0^\circ$; data from transonic bump.

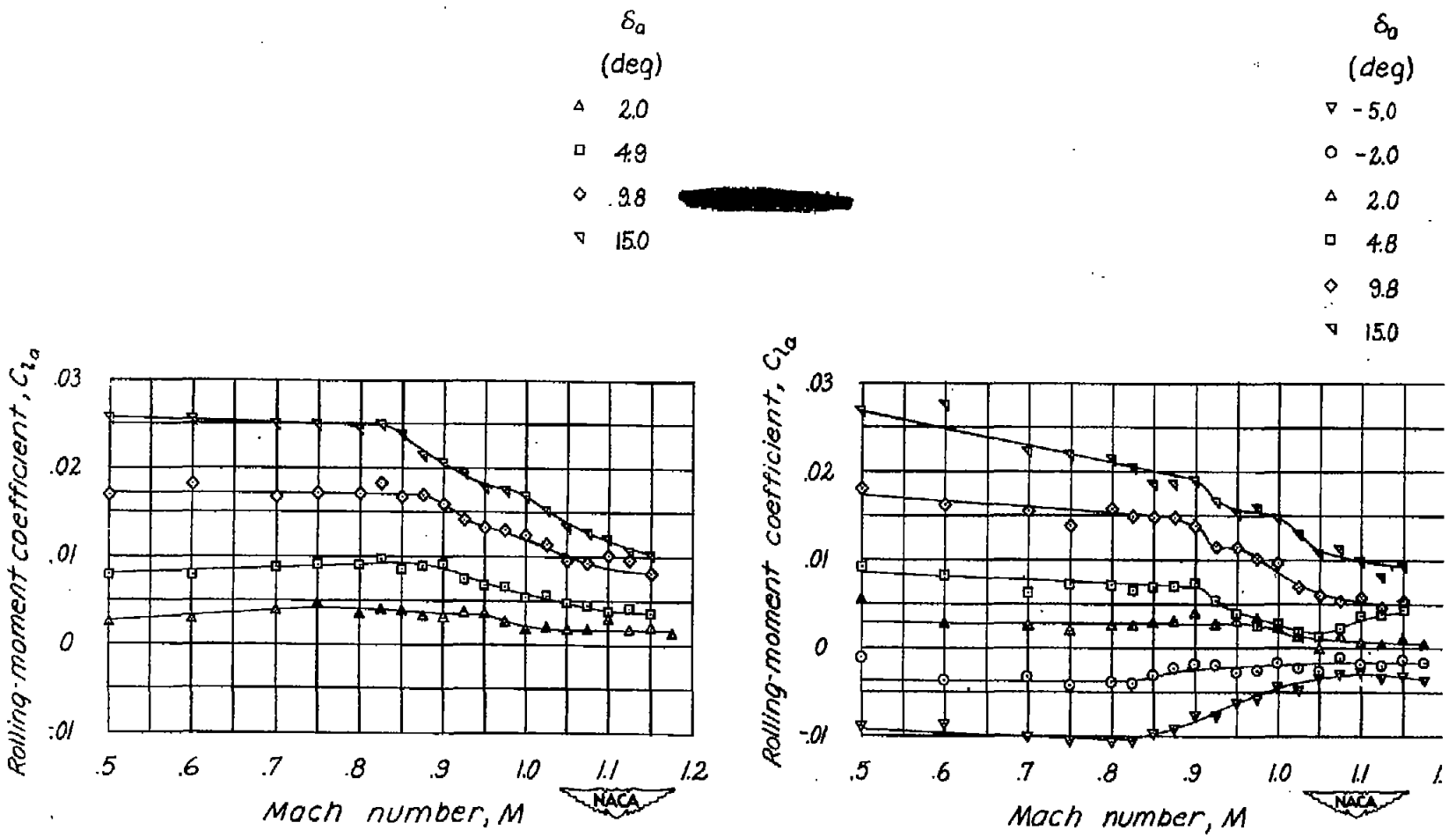

(a) $\alpha = 0^\circ$.

(b) $\alpha = 3.4^\circ$.

Figure 17.- Variation of rolling-moment coefficient with Mach number for a 0.20-chord flat-sided aileron. t = 0.50; data from transonic bump.

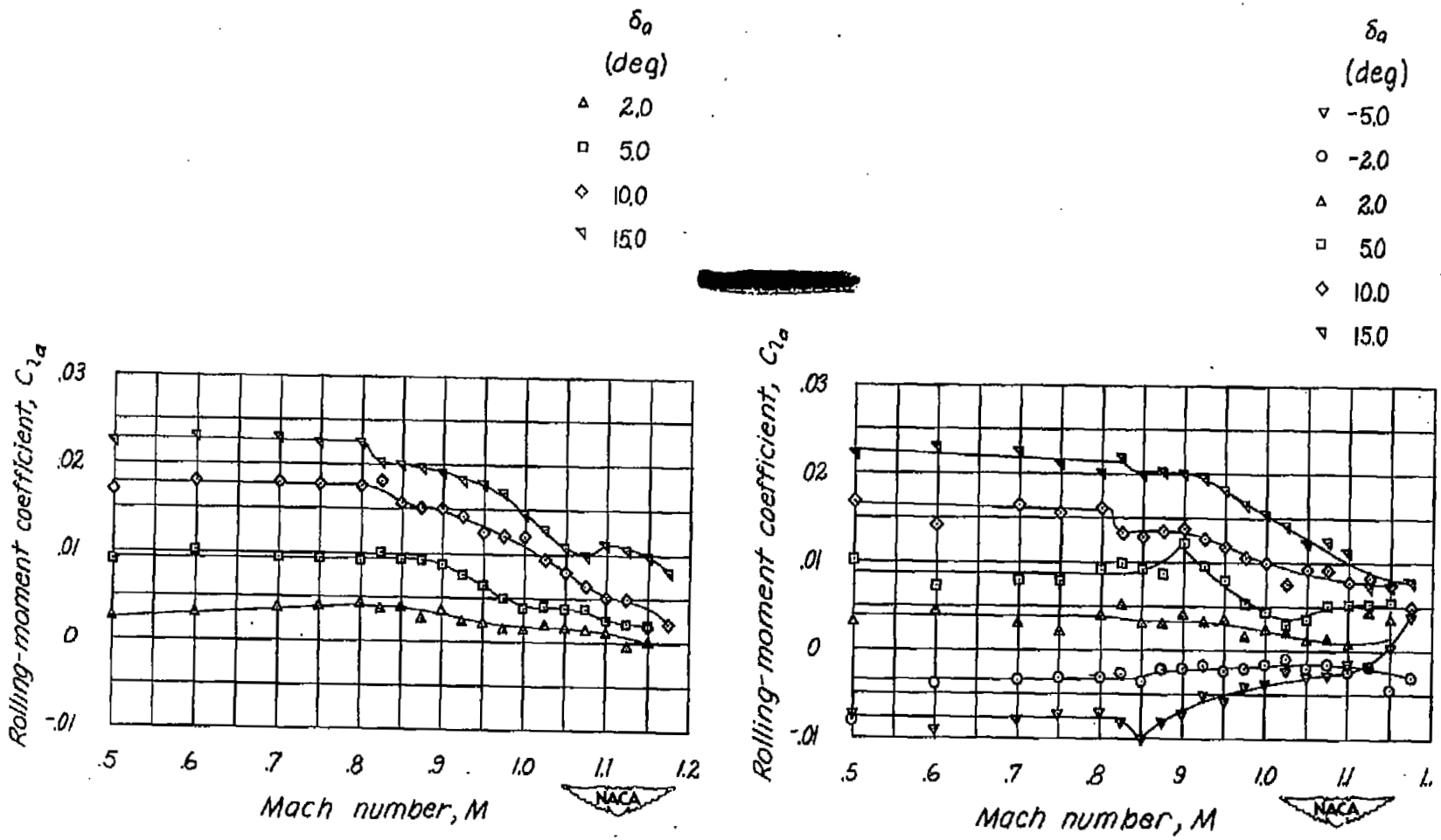

(a) $\alpha = 0°$.

(b) $\alpha = 3.5°$.

Figure 18.- Variation of rolling-moment coefficient with Mach number for a 0.20-chord flat-sided aileron. t = 0.37; data from transonic bump.

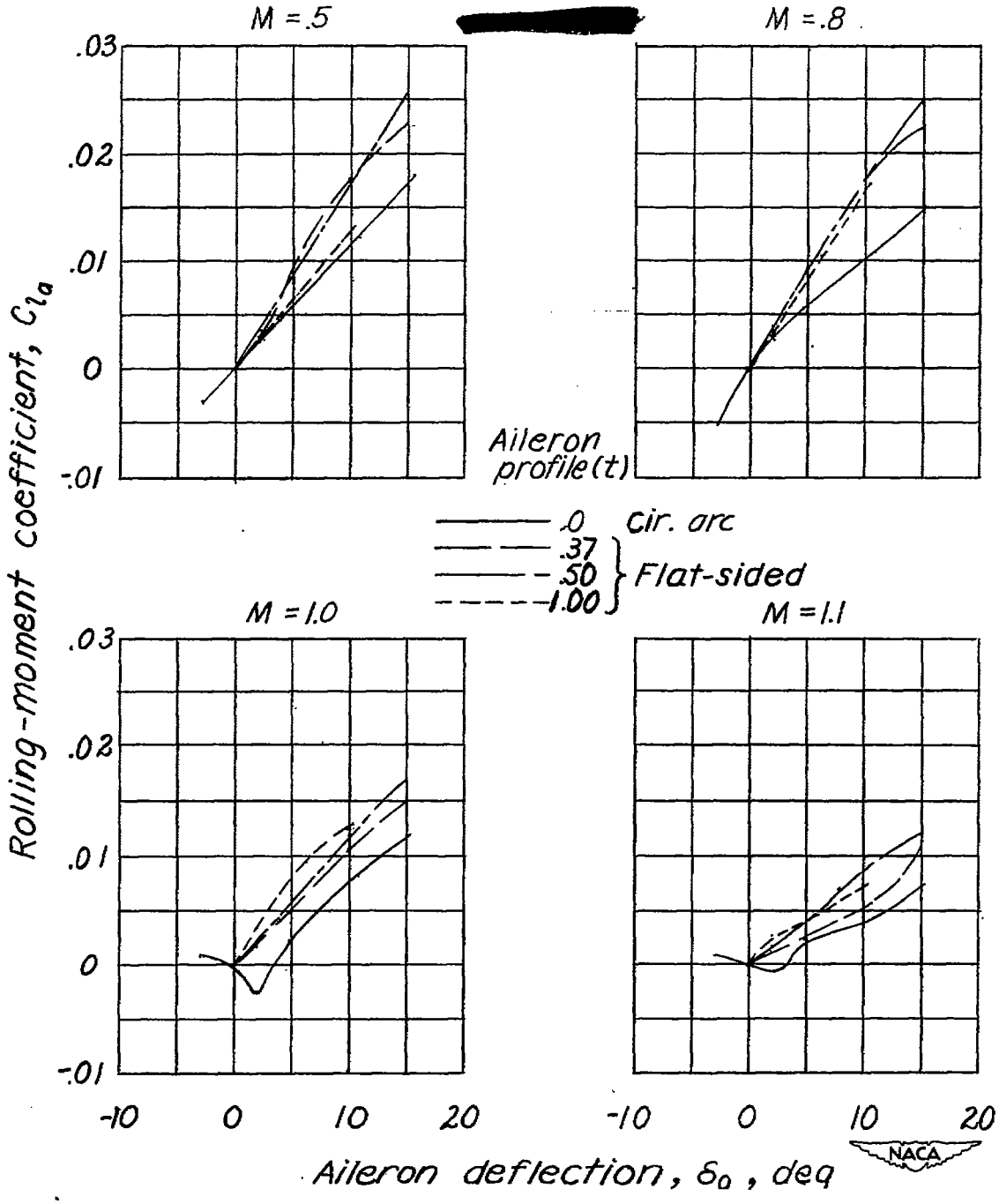

Figure 19.- The effect of aileron profile on the rolling-moment characteristics. $\alpha = 0^\circ$; data from transonic bump.